Tryptophan Residues Flanking the Second Transmembrane Helix (TM2) Set the Signaling State of the Tar Chemoreceptor†

Roger R. Draheim, Arjan F. Bormans, Run-zhi Lai, and Michael D. Manson*

Department of Biology, 3258 TAMU, Texas A&M University, College Station, Texas 77843

Received May 20, 2004; Revised Manuscript Received November 8, 2004

ABSTRACT: The chemoreceptors of *Escherichia coli* are homodimeric membrane proteins that cluster in patches near the cell poles. They convert environmental stimuli into intracellular signals that control flagellar rotation. The functional domains of a receptor are physically separated by the cell membrane. Chemoeffectors bind to the extracellular (periplasmic) domain, and the cytoplasmic domain mediates signaling and adaptation. These two domains communicate through the second transmembrane helix (TM2) that connects them. In the high-abundance receptors Tar and Tsr, TM2 is flanked by tryptophan residues, which should localize preferentially to the interfacial zone between the polar and hydrophobic layers of the phospholipid bilayer. To investigate the functional significance of the Trp residues that flank TM2 of Tar, we used site-directed mutagenesis to generate the W192A and W209A substitutions. The W192A protein retains full activity in vivo and in vitro, but it increases the K_i for aspartate in the in vitro assay 3-fold. The W209A replacement eliminates receptor-mediated stimulation of CheA in vitro, and it leads to an increased level of adaptive methylation in vivo. This phenotype in some respects mimics the changes seen upon binding aspartate. Since the W209A substitution may cause the C-terminus of TM2 to protrude farther into the cytoplasm, these results reinforce the hypothesis that aspartate binding causes a similar displacement. Moving Trp to each position from residue 206 to residue 212 generated a wide variety of Tar signaling states that are generally consistent with the predictions of the piston model of transmembrane signaling. None of these receptors was completely locked in one signaling mode, although most showed pronounced signaling biases. Our findings suggest that the Trp residues flanking TM2, especially Trp-209, are important in setting the baseline activity and ligand sensitivity of the Tar receptor. We also conclude that the Tyr-210 residue plays at least an auxiliary role in this control.

Escherichia coli performs chemotactic migrations in response to a wide variety of environmental stimuli, including changes in pH (*1*), temperature (*2*), redox potential (*3*, *4*), amino acids (*5*), sugars (*6*), small peptides (*7*), and certain noxious organic compounds and divalent cations (*1*). Cells swim up gradients of attractant stimuli and down gradients of repellent ones. To do so, cells bias a three-dimensional random walk of alternating smooth swims (runs) and reorienting tumbles by selectively lengthening runs in the favorable direction (*8*).

The signal transduction pathway that directs the biased random walk controls the direction of flagellar rotation. Each of the five members of a family of homodimeric chemoreceptors detects a specific set of stimuli. These receptors normally activate the histidine protein kinase CheA (*9*), which is coupled to the receptors via the adapter protein CheW. CheA autophosphorylates, and the phosphoryl group is then transferred to the response regulator CheY (*10*). CheY-P binds to FliM in the flagellar motor to promote clockwise (CW)[1] rotation of the flagella (*11*, *12*).

Counterclockwise (CCW) motor rotation allows the flagellar filaments, which are left-handed helices, to coalesce into a bundle that propels the cell in a run (*13*). CW rotation of one or more flagella disrupts the bundle and generates a tumble (*14*). The relative activities of CheA and the CheY-P phosphatase, CheZ, establish the ratio of CheY to CheY-P within the cell, and hence the frequency of tumbling (*10*, *15*).

The conformational changes induced by an attractant stimulus convert a receptor from a stimulator of CheA activity into an inhibitor (*16*). The resulting drop in CheY-P, which is accelerated by CheZ, suppresses tumbling and lengthens the average run. Inhibition of CheA activity is reversed by covalent methylation of the cognate receptor (*17*). Methylation is also facilitated by a transient decrease in the level of the active, phosphorylated form of the CheB methylesterase (*18*), which is another substrate for phosphotransfer from CheA (*10*).

Tar functions as the aspartate chemoreceptor in *E. coli* (*19*). The crystal structures of the periplasmic ligand-binding domains of Tar from *Salmonella enterica* serovar Typhimurium (*20*, *21*) and *E. coli* (*22*) show that each monomeric

† This work was supported by a grant from the National Institutes of Health (Grant GM39736 to M.D.M.).

* To whom correspondence should be addressed. Tel: (979) 845−5158. Fax: (979) 845-2981. E-mail: mike@mail.bio.tamu.edu.

[1] Abbreviations: TM1, first transmembrane helix; TM2, second transmembrane helix; CW, clockwise; CCW, counterclockwise; H1, periplasmic helix one; H4, periplasmic helix four; WALP peptide, tryptophan-flanked poly-(Ala-Leu) peptide; Tris, Tris(hydroxymethyl)-aminomethane; EDTA, ethylenediaminetetraacetic acid; DTT, dithiothreitol; TCA, trichloroacetic acid; 5-IAF, 5-iodoacetamidofluorescein.

10.1021/bi048969d CCC: $30.25
Published on Web 12/31/2004

unit of the functional homodimer (*23*, *24*) consists of four antiparallel α helices that form a quasi four-helix bundle. Sulfhydryl reactivity experiments (*25*−*28*) demonstrate that the transmembrane regions (TM1 and TM2) flanking the periplasmic domain are extensions of the periplasmic helices H1 and H4. Aspartate binds at either of two rotationally symmetrical sites at the dimer interface, each of which contains residues from H1 of one subunit and H4 of the opposing subunit. *E. coli* Tar exhibits half-of-sites binding such that, under most conditions, only one molecule at a time of aspartate associates with a given dimer (*29*). Aspartate binding is proposed to generate a downward vertical displacement of a few angstroms in one H4-TM2 helix relative to its H1-TM1 helix partner (*28*, *30*−*34*). This movement should also reposition TM2 relative to the plane of the cell membrane.

Tryptophan residues in transmembrane helices localize preferentially to the interfacial regions of phospholipid bilayers (*35*). A glycosylation-site mapping technique (*36*) implicated Trp residues in determining the vertical position of a synthetic poly-Leu transmembrane helix oriented roughly perpendicular to the membrane. Shifting the location of Trp residues within the peptide repositioned the helix to allow Trp to reside within the interfacial zone (*37*). Also, synthetic peptides consisting of an Ala-Leu core of different lengths flanked by Trp (WALP peptides) interact in a characteristic manner with phospholipid bilayers (*38*). The flanking Trp residues exhibit a strong tendency to remain within the interfacial region regardless of the length of hydrophobic mismatch (*39*), indicating that they are significant determinants in governing how a transmembrane helix interacts with the membrane.

TM2 of *E. coli* Tar consists of a largely aliphatic core of sixteen residues bounded by a Trp residue at each end. It thus resembles a WALP peptide. This striking similarity prompted us to examine whether these Trp residues modulate the signaling state of Tar. We report here the effects of the residue substitutions W192A and W209A on the function of Tar in vivo and in vitro. We then describe the results obtained when Trp was moved from position 209 to each of positions 206 through 212. Our findings emphasize the crucial role of Trp-209 in regulating the activity of the Tar receptor. By extension, they suggest that the aromatic residues that are conserved in many homodimeric chemoreceptors and transmembrane sensor kinases may play a similarly important role. Finally, we propose that our results support a piston model for transmembrane signaling by this entire set of bacterial proteins.

MATERIALS AND METHODS

Bacterial Strains and Plasmids. Strain RP3098 (*40*) is a Δ *(flhD-flhB)4* derivative of the *E. coli* K-12 strain RP437 (*41*). Strain VB13 (*42*) is a *thr*$^+$ *eda*$^+$ Δ*tsr7201 trg*::Tn*10* Δ*tar-tap5201* version of RP437. Plasmid pRD100 was created by cloning the PCR-amplified *tar* gene from plasmid pMK113 (*43*) into pBAD18 (*44*), using flanking *Eco*RI and *Hin*dIII restriction sites. Plasmid pRD200 was made by adding an in-frame coding sequence to the 3′ end of *tar*. This sequence encodes a seven-residue linker (GGSSAAG) (*45*) and a C-terminal V5 epitope tag (GKPIPNPLLGLDST) (*46*). The *Bam*HI site in the *tar* promoter region of pMK113 was also removed to restore the wild-type sequence. Plasmid pRD300 is identical to pRD100 except for the addition of the in-frame coding sequence for the seven-residue linker and C-terminal V5 tag. Mutations were introduced into *tar* in these plasmids using standard site-directed mutagenesis techniques (Stratagene).

Observation of Swimming Cells. Cells were inoculated from a single colony on Luria Broth agar (*47*) containing 50 μg/mL ampicillin into 25 mL of tryptone broth (*47*) supplemented with 50 μg/mL ampicillin. Cultures were swirled at 32 °C until they reached an optical density at 600 nm of ∼0.7, at which time a large majority of cells were highly motile. Cells were diluted 1:50 into tethering buffer [10 mM potassium phosphate (pH 7.0), 100 mM NaCl, 10 μM EDTA, 20 μM L-methionine, 20 mM sodium lactate, 20 μg/mL chloramphenicol] and observed at 1000× magnification under phase contrast using an oil immersion 100× objective and Olympus BH-2 microscope. Ten separate fields, each traversed by five to ten cells during the approximately 30 s observation period, were analyzed for each strain. A subjective assessment was made of whether individual cells were running and tumbling (R cells), smooth swimming (S cells), or primarily tumbling (T cells).

Observation of Tethered Cells. Cultures were grown as described above and harvested by centrifugation after the addition of chloramphenicol to a final concentration of 30 μg/mL to prevent regrowth of flagella after shearing. Cells were resuspended in 25 mL of tethering buffer containing 30 μg/mL chloramphenicol and exposed to six 10-s intervals of agitation at high speed in a 50 mL stainless steel cup of a Waring blender. Bouts of blending were separated by 15 s to allow cooling. Cells were then pelleted by centrifugation and resuspended in 5 mL of tethering buffer containing chloramphenicol. These cells were kept on ice until needed, when 20 μL of cell suspension was mixed with 20 μL of a 200-fold dilution of anti-flagellar filament antibody. This entire volume was loaded within a peripheral ring of Apiezon-L grease on a 12 mm diameter round coverslip. After incubation for 20 min at room temperature, coverslips were affixed to a flow chamber (*48*), and nontethered cells were removed by passing several milliliters of tethering buffer through the chamber. Cells were observed at 1000× magnification, as described above. Enough fields were videotaped for ∼1 min apiece to ensure that at least 30 freely rotating cells could be analyzed for each strain.

Rotational behavior was assessed during video playback. Cells were divided into three categories: cells that turned their flagella only CCW, cells that exhibited only a few, brief reversals to CW flagellar rotation, and cells that reversed often and/or rotated for extended intervals both CCW and CW.

C*hemotaxis Swarm Assays*. Swarm assays were run as described (*45*), with minor modifications. Briefly, semisolid agar contained 0.325 g/L Difco BactoAgar in motility medium [10 mM potassium phosphate (pH 7.0), 1 mM $(NH_4)_2SO_4$, 1 mM $MgSO_4$, 1 mM $MgCl_2$, 1 mM glycerol, 90 mM NaCl] supplemented with 20 μg/mL L-threonine, L-histidine, L-methionine, and L-leucine and 1 μg/mL thiamine. Ampicillin was present at 25 μg/mL. Aspartate and maltose were added to a final concentration of 100 μM. Swarm plates were incubated at 30 °C. Once visible swarm

rings formed, their diameter was measured every 2 h, and the rate of ring expansion was expressed in mm/h.

Protein Preparation. We employed the protocol of Gegner et al. (*49*), with minor modifications. Strain RP3098 containing pRD100 or one of its derivatives was used for production of receptor-containing membranes. Tar expression was induced by addition of L-arabinose to a final concentration of 0.2% (w/v). CheY was purified using the method described by Hess et al. (*50*).

Receptor-Linked CheA Kinase Assay. We employed a slightly modified version of the receptor-coupled phosphorylation assay described by Borkovich and Simon (*51*). Tar-containing membranes (20 pmol of Tar) and CheY (500 pmol) were added to CheA (5 pmol) and CheW (20 pmol), which were incubated overnight on ice in a total volume of 9 μL of fresh phosphorylation buffer [50 mM Tris-HCl, 50 mM KCl, 5 mM $MgCl_2$, 2 mM DTT (pH 7.5)]. Aspartate was added to the desired final concentration while the same total volume was maintained. This mixture was then held at room temperature for 4 h. The reaction was initiated by addition of 1 μL of [γ-^{32}P]-ATP (3000 Ci/mmol NEN# BLU502A) diluted 1:1 with 10 mM unlabeled ATP. Reactions were terminated by adding 40 μL of 2X SDS−PAGE loading buffer containing 25 mM EDTA. Production of CheY-^{32}P was determined to be linear through 20 s and to be proportional to the amount of receptor present over a range from 5 to 40 pmol (data not shown). Ultimately, we used 20 pmol in each reaction because this concentration is in the middle of the linear range, allowing us to measure increases or decreases in production of CheY-P accurately. Analysis of the aspartate-induced titration curves was performed according to a previously described method (*52*), using KaleidaGraph v3.6 software and the Hill equation to determine the cooperativity of inhibition by aspartate. We calculated the concentration of free aspartate by performing a series of iterations in which we used the uncorrected aspartate values to determine an approximate K_i, which was then used to determine free aspartate (total minus bound) to calculate a new K_i. We performed consecutive iterations until no change in K_i or the Hill coefficient was observed. The uncertainties in the estimates of the K_i and Hill coefficients represent the standard deviation of the mean, with $n \geq 3$.

Determination of the Methylation State of Receptors in Vivo. We adapted our methylation assay from Weerasuriya et al. (*42*). To determine levels of receptor methylation, VB13 cells harboring plasmid pRD200 or one of its mutant derivatives were grown to an OD_{590nm} of 0.6 in 10 mL of tryptone broth (*47*). Cells were harvested by centrifugation and washed three times with 10 mM potassium phosphate, 0.1 mM EDTA (pH 7.0) and finally resuspended in 5 mL of 10 mM potassium phosphate (pH 7.0), 10 mM sodium lactate, and 200 μg/mL chloramphenicol. One-milliliter aliquots of cells were transferred to 10-mL scintillation vials and incubated with shaking for 10 min at 32 °C. Following addition of L-methionine to 2 μM, cells were incubated for an additional 30 min. In some samples, aspartate or $NiSO_4$ was added to 100 mM and 10 mM, respectively, and the cells were incubated for an additional 20 min. Control reactions received an equal volume of buffer. Reactions were terminated by addition of 100 μL of ice-cold 100% TCA and then incubated on ice for 15 min. Proteins were pelleted by centrifugation at 13000*g* and subsequently washed with 1% TCA and acetone. The proteins were resuspended in 200 μL of 2X SDS-loading buffer. A 10-μL aliquot of each sample was loaded into a 7.5% SDS gel. Following electrophoresis, the proteins were transferred to nitrocellulose and subjected to immunoblotting and visual detection by antibody against the V5 epitope (Invitrogen), using goat-anti-mouse conjugated with alkaline phosphatase (Bio-Rad) as the secondary antibody.

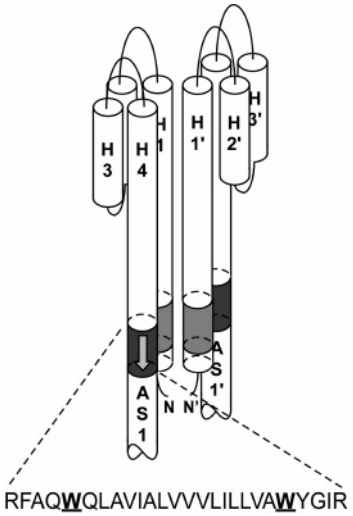

FIGURE 1: Schematic representation of the periplasmic and transmembrane (TM) domains of the *E. coli* Tar chemoreceptor. TM1 and TM2 are represented as light and dark shaded areas, respectively. Upon binding aspartate, TM2 of one monomer is proposed to be displaced toward the cytoplasm, thereby repositioning TM2 relative to the phospholipid bilayer. The extent of TM2 shown is based on sulfhydryl-reactivity studies with *S. typhimurium* Tar and 5-IAF (*56*). The Trp-192 and Trp-209 residues, which are believed to reside within the interfacial regions of the cytoplasmic membrane, are in bold face.

RESULTS

Substitution of Trp Residues Flanking TM2 with Ala. The position of TM2 of Tar relative to TM1 is a crucial factor in transmembrane signal transduction (*28*, *30*−*34*). Inspired by the demonstrated role of Trp residues in positioning transmembrane helices, we decided to assess the role of the Trp-192 and Trp-209 residues that flank TM2 in modulating the signaling state of the receptor (Figure 1). We generated mutant versions of Tar containing the W192A or W209A substitution as well as the W192A-W209A (WAWA) double substitution. We chose Ala as the replacement residue because it removes the amphipathic character of Trp, does not introduce charge or polar character, and minimizes the probability of introducing steric hindrance or helix disruption. We made these changes in plasmid pRD200, which expresses fully functional Tar with a C-terminal V5 epitope tag (see below).

Chemotactic Behavior of Cells Expressing Trp-Substituted Receptors. We expressed both wild-type and mutant Tar proteins in the transducer-depleted (ΔT) strain VB13, which retains the redox receptor Aer. The chemotactic behavior of these cells was tested in aspartate, maltose, and glycerol motility agar, the last of which allows an assessment of aerotaxis in the absence of any specific Tar chemoeffector. Substitution of Trp-192 with Ala decreased the rate of swarm-ring expansion in aspartate and maltose motility agar

Table 1: Swarm Behavior of VB13 (ΔT) Cells Harboring Wild-Type and Mutant Plasmid-Borne *tar* Genes

	swarm expansion rates[a]		
receptor	aspartate	maltose	glycerol
WT	1.72 ± 0.14	0.87 ± 0.04	0.55 ± 0.04
W192A	1.49 ± 0.11	0.71 ± 0.10	0.46 ± 0.05
W209A	0.67 ± 0.00	0.50 ± 0.03	0.38 ± 0.01
WAWA	0.98 ± 0.07	0.57 ± 0.09	0.43 ± 0.03

[a] The rate at which the swarm diameter increased was measured in mm/h, as described in Materials and Methods. The error represents the standard deviation of three independent assays.

to 85% of the wild-type rate, a statistically insignificant difference (Table 1). In contrast, substitution of Trp-209 with Ala decreased the rate of ring migration to 45% and 60% of the wild-type rate in aspartate and maltose semisolid agar, respectively. When both Trp-192 and Trp-209 were substituted with Ala, intermediate expansion rates of 60% and 70% of the wild-type rate were observed. All mutants formed aerotaxis rings in agar containing only glycerol, with swarms expanding at 85%, 70%, and 80% of the wild-type rate for the W192A, W209A, and WAWA mutants, respectively.

The swarms made by cells expressing either W209A or WAWA Tar formed significantly sharper rings on aspartate plates (data not shown). This result suggests that these cells may respond differently to the aspartate gradient produced by the expanding colony.

Stimulation of CheA Activity by Trp-Substituted Receptors in Vitro. Any inherent changes in the ability of the mutant receptors to stimulate CheA activity or to alter their activity in response to aspartate could be partially masked by adaptive methylation. Performing in vitro assays using purified components in the absence of CheR and CheB avoids this complication. We therefore isolated inner-membrane vesicles from cells in which wild-type or mutant Tar proteins were expressed at high levels from an arabinose-inducible, plasmid-borne *tar* gene in strain RP3098, which lacks all flagellar, motility, and chemotaxis proteins. These membranes were then used in an in vitro assay for receptor-coupled CheA kinase activity (*51*). In these membranes, all of the Tar present is in the unmodified state in which the protein is originally translated. The four sites of covalent methylation are correspondingly occupied by two Gln residues and two Glu residues (the QEQE form of the receptor). Tar constituted between 50% and 65% of the total protein in membrane preparations for the wild-type and mutant receptors (data not shown). Thus, all of the mutant proteins are reasonably stable.

Receptor−CheW−CheA complexes containing wild-type Tar produced produced 44 ± 1 pmol of CheY-P in 20 s (Table 2). Complexes containing the W192A mutant Tar produced 44 ± 6 pmol in 20 s, similar to the wild-type receptor. The W209A substitution, either by itself or in combination with W192A, eliminated receptor-mediated stimulation of CheA activity almost completely. This behavior resembles that of the previously described "lock-off" disulfide-scanning mutants (*31*), in which no modulation of CheA activity was detected. We concluded that the relatively good swarming of cells expressing Tar W209A or WAWA might depend on compensation through adaptive methylation.

Aspartate Inhibition of Receptor-Coupled CheA Activity. To examine the role of the Trp-192 residue in transmembrane signaling in more detail, we compared aspartate inhibition of the CheA kinase activity in vitro stimulated by the wild-type and W192A Tar receptors. We used the multisite Hill equation to draw a best-fit curve to the data (Figure 2), as previously described (*52*). The wild-type Tar−CheA−CheW complex had a K_i for aspartate of 7 ± 1 μM. Complexes containing W192A had a 3-fold increase in K_i to 22 ± 1 μM. The mutation did not appear to alter the cooperativity involved in aspartate-induced inhibition of CheA kinase activity, with the Hill coefficients being 1.8 ± 0.1 to 2.0 ± 0.2 for the wild-type and W192A proteins, respectively.

Table 2: CheA Kinase-Stimulating Activity of Trp-to-Ala Tar Proteins[a]

receptor	pmol of CheY-P produced
none	0.24 ± 0.02
WT	44.37 ± 1.26
W192A	44.55 ± 5.80
W209A	0.26 ± 0.02
WAWA	0.48 ± 0.07

[a] CheA kinase activity was measured as the accumulation of CheY-P after 20 s, as described in Materials and Methods. Activities were calculated by averaging the values obtained for at least three independent membrane preparations assayed in duplicate. The error represents the standard deviation of the mean for these measurements.

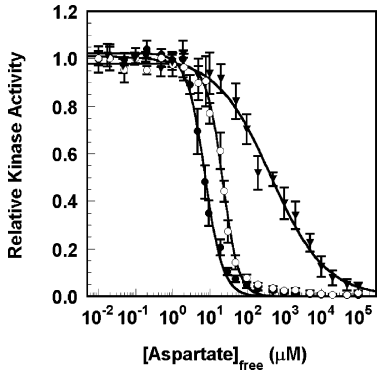

FIGURE 2: Aspartate inhibition of receptor-coupled CheA activity for wild-type, W192A Tar, and W211 Tar. The data are shown as closed circles, open circles, and closed triangles, respectively. The inhibition assays were performed as described in Materials and Methods. Each data point represents the mean of at least six total reactions from at least three independently isolated receptor-containing vesicle preparations. The best-fit curve (solid line) is based on the cooperative multisite Hill model (*52*). The error bars represent the standard deviation of the mean, with $n \geq 3$.

Effect of Trp Substitutions on in Vivo Methylation of Tar. All of the Trp-substituted Tar proteins supported chemotactic swarming in aspartate and maltose semisolid agar to a significant degree. In view of the very low activity of the W209A and WAWA proteins in the in vitro CheA-stimulation assay, we decided to test whether compensating changes in receptor methylation restored chemotaxis. We expressed V5-tagged wild-type and mutant Tar proteins in the ΔT strain VB13 and monitored the level of Tar methylation in the absence and presence of various chemoeffectors. To provide a scale for comparing the levels of methylation, we transformed strain RP3098 with derivatives of plasmid pRD300 that produce V5-tagged Tar proteins in which the methylation sites are all Gln (QQQQ), all Glu (EEEE), or in the unmodified (QEQE) form. During SDS−PAGE, the QQQQ receptor should migrate fastest, like the fully methylated Tar protein, the unmethylated EEEE receptor should run slowest,

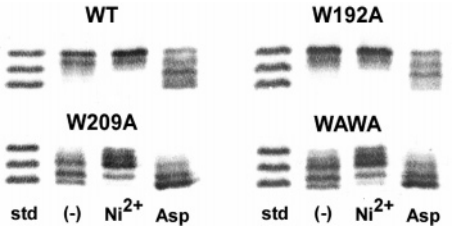

FIGURE 3: Changes in the in vivo methylation of wild-type and Trp-to-Ala (WA) mutant Tar proteins in VB13 (ΔT) cells exposed to aspartate and Ni^{2+}. Migration rate is affected by the level of methylation, with the more highly methylated forms moving faster. As migration standards, the EEEE, QEQE, and QQQQ forms of Tar were loaded on the leftmost lane. The QEQE and QQQQ forms of Tar migrate like doubly methylated and quadruply methylated Tar. Chemoeffectors were added to the cells as 10 mM $NiSO_4$ (repellent) and 100 mM aspartate (attractant). Equal amounts of total protein were loaded on each lane.

and the QEQE receptor should migrate to an intermediate position (Figure 3).

With wild-type Tar proteins produced in VB13 cells, we observed two distinct bands that correspond to unmethylated and singly methylated species. Addition of a saturating concentration of aspartate (100 mM) led to a substantial increase in methylation, whereas a saturating amount (10 mM) of the repellent $NiSO_4$ caused a slight decrease. The methylation patterns of Tar W192A were nearly identical to those of the wild type.

The Tar W209A or Tar W192A W209A receptors expressed in strain VB13 showed a dramatic increase in basal methylation. This result could explain why these proteins, which fail to stimulate CheA kinase activity in vitro when they are in the QEQE form, support chemotactic swarming. Apparently, methylation can compensate for the low CheA-stimulating activity of a receptor that lacks the cytoplasmic interfacial anchor for TM2, just as it restores activity to attractant-bound wild-type receptor.

Addition of 100 mM aspartate produced a further increase in methylation of the W209A and WAWA receptors, which exhibited higher levels of methylation than the aspartate-adapted wild-type and W192A receptors. Similarly, Ni^{2+} at 10 mM decreased methylation below the baseline level for the W209A and WAWA proteins, but the methylation was greater than for nickel-adapted wild-type or W192A Tar. Thus, adaptive methylation and demethylation occur in the absence of Trp-209, but with the absolute extent of methylation shifted to a level higher than that of wild-type Tar in naive, attractant-adapted and repellent-adapted cells.

Repositioning the Cytoplasmic Interfacial Trp Residue Alters Chemotactic Behavior. Since replacement of Trp-209 with Ala shifted Tar signaling in a similar manner as binding of an attractant ligand, we wondered whether the output of Tar could be more subtly modulated by moving this Trp residue in one-residue increments in the N-terminal and C-terminal directions. We began with the Tar W209A protein and introduced Trp at each position within one helical turn of position 209. These mutants were named W206 through Tar W212 according to the position at which Trp replaced the original residue. W209 is the wild-type receptor.

We expressed these proteins in strain VB13 and analyzed their behavior in aspartate, maltose, and glycerol semisolid agar plates (Table 3). Three swarm phenotypes were observed. The first, seen with the W207 and W211 strains,

Table 3: Swarm Behavior of VB13 (ΔT) Cells Harboring Wild-Type and Mutant Plasmid-Borne *tar* Genes[a]

receptor[b]	aspartate swarm rate	maltose swarm rate	glycerol swarm rate
W206	0.88 ± 0.12	0.71 ± 0.13	0.42 ± 0.04
W207	1.50 ± 0.04	0.71 ± 0.06	0.50 ± 0.04
W208	0.31 ± 0.04	0.29 ± 0.04	0.33 ± 0.01
W209 (WT)	1.72 ± 0.14	0.87 ± 0.04	0.55 ± 0.04
W210	1.03 ± 0.08	0.77 ± 0.05	0.39 ± 0.01
W211	1.81 ± 0.14	0.78 ± 0.02	0.38 ± 0.00
W212	0.09 ± 0.04	0.18 ± 0.03	0.12 ± 0.01

[a] The rate at which the swarm diameter expanded was measured in mm/h as described in Materials and Methods. [b] The mutant receptors Tar W206 through Tar W212 were named according to the position at which the original residue in the Tar W209A protein was replaced by Trp. This manipulation placed a single Trp residue near the cytoplasmic end of TM2 at the specified position in each mutant receptor.

Table 4: Effect of Repositioning of Trp-209 on CheA Kinase Activity[a]

receptor[b]	pmol of CheY-P produced
W206	0.42 ± 0.04
W207	0.61 ± 0.04
W208	0.80 ± 0.06
W209 (WT)	44.37 ± 1.26
W210	0.21 ± 0.02
W211	40.01 ± 7.07
W212	0.67 ± 0.11

[a] CheA kinase activity was measured as the accumulation of CheY-P after 20 s, as described in Materials and Methods. [b] The W206 through W212 receptors are described in the footnote to Table 3.

was like wild type on all three plates. Cells expressing Tar W206 and Tar W210 formed swarms on aspartate plates like those of cells expressing Tar W209A, with very narrow, sharp chemotactic rings and rates of migration approximately half those of cells expressing wild-type Tar. Finally, cells expressing the W208 and W212 proteins failed to produce significant swarms on any of the three plates, looking just like VB13 cells containing the vector plasmid without a *tar* gene.

In Vitro Stimulation of CheA Activity by Receptors with Repositioned Trp Residues. We next analyzed the ability of the W206 through W212 receptors to stimulate CheA in vitro (Table 4). Only W209 (wild type) and W211 Tar stimulated CheA activity. Complexes containing Tar W211 produced 40 ± 7 pmol of CheY-P in 20 s and were not significantly different from wild-type Tar. We then examined the ability of aspartate to inhibit stimulation of CheA kinase by W211 Tar (Figure 2). The K_i value determined was 430 ± 50 μM, about 60-fold higher than the wild-type value of 7.0 ± 1 μM. The calculated Hill coefficient dropped to 0.6 ± 0.1 from the wild-type value of 1.8 ± 0.1.

In Vivo Methylation of Receptors with Repositioned Trp Residues. To determine whether methylation compensates for the signaling biases introduced by the repositioned Trp residues, we analyzed the level of methylation of the mutant receptors (Figure 5). Tar W211 showed wild-type levels of methylation in the absence of chemoeffectors and after adaptation to saturating concentrations of aspartate and Ni^{2+}. The W206, W207, and W210 receptors produced methylation patterns very similar to those of the W209A and WAWA proteins. The differences in the swarm phenotypes of cells expressing W206 versus W207 Tar could be due to the

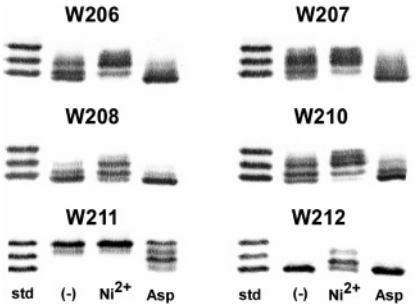

FIGURE 4: Changes in in vivo methylation of wild-type and repositioned-Trp mutant Tar proteins in VB13 (ΔT) cells exposed to aspartate or Ni^{2+}. Analysis was as in the caption for Figure 3.

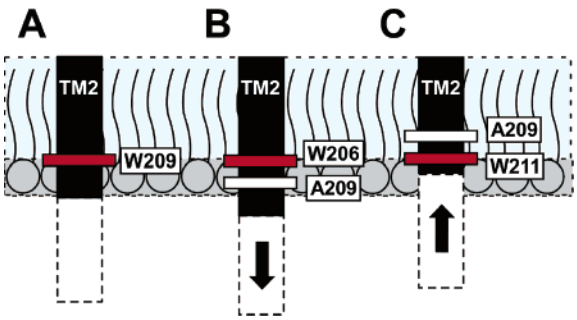

FIGURE 5: Model for the role of cytoplasmic interfacial Trp residue in setting the activity level of Tar. TM2 is represented by a dark rectangle. Trp residues are shown as red boxes, and white boxes represent the introduced Ala-209 residue. In the wild-type receptor (A), Trp-209 is predicted to reside within the cytoplasmic interfacial region (*56*). Upon repositioning the cytoplasmic interfacial Trp residue into the hydrophobic core, we predict a displacement of TM2 toward the cytoplasm, as represented by the downward-directed arrow in (B). Upon repositioning a Trp residue toward the cytoplasm, we predict a displacement of TM2 into the membrane, as indicated by the upward-directed arrow in (C).

greater severity of the signaling bias of the former, since the methylation levels of W207 Tar were intermediate between the wild-type and W206 proteins, and closer to the former. Tar containing Trp-208 or Trp-212 exhibited extreme overmethylation in the absence of chemoeffectors, yet these proteins partially demethylated after the addition of Ni^{2+}. Thus, even these extremely CCW-biased mutants are not totally blind to repellent stimuli, and therefore the W208 and W212 receptors cannot be "locked" in one conformation. It remains to be seen whether they can mediate a CW (tumbly) response to nickel.

Motility Patterns of Cells Expressing Mutant Tar Receptors. Our prediction was that compensatory methylation enables mutant cells to achieve a baseline run-tumble swimming pattern that is compatible with chemotaxis in every case except for strains expressing the W208 or W212 Tar protein. To confirm, we observed the swimming behavior of all strains using phase contrast microscopy. Strain VB13 harboring the vector plasmid pBR322 (*53*) or pRD200 carrying a *tar* gene encoding the W208 or W212 protein appeared to be almost entirely smooth swimming (Table 5), whereas VB13 cells carrying any other of the mutant *tar* genes tumbled with about the same frequency as cells containing the tar^+ control plasmid.

To measure the rotational biases of the flagellar motors of the various mutants directly, we examined tethered cells (Table 5). As expected, VB13 cells containing the vector plasmid never reversed. The same was true for cells expressing the W212 Tar protein, and of 45 cells expressing W208 Tar, only two reversed. In contrast, the fraction of reversing cells for the other mutants was similar to the fraction of VB13 cells expressing wild-type Tar that reversed.

Table 5: Motile Behavior of VB13 Cells Expressing Wild-Type or Mutant Tar Proteins

		tethered cells[c]		
receptor[a]	swimming cells[b]	cells with flagella that rotate only CCW	cells with CCW-biased flagella that occasionally reverse	cells with flagella that reverse frequently or show extended CCW and CW rotation
wild type	R, s, T	5	2	23
none	S	33	0	0
W192A	R, S, t	12	2	24
W209A	R, s, T	5	0	28
WAWA	R, s, T	9	1	20
W206	R, S, T	4	1	27
W207	R, S, t	4	2	23
W208	r, S	45	0	2
W210	R, s, T	14	3	18
W211	R, S, T	6	5	25
W212	r, S	41	0	0

[a] Tar proteins are designated using the nomenclature described in the text and in footnote *b* of Table 3. None indicates that vector plasmid without a *tar* gene insert was present. [b] Ten fields of cells swimming in TB medium at room temperature were observed for about 30 s each. R, S, and T represent cells that were running and tumbling, smooth swimming, and primarily tumbling, respectively. Uppercase letters indicate that a large fraction of the cells observed behaved in the manner indicated. Lowercase letters indicate that only a few cells exhibited the behavior indicated. [c] Tethered cells were prepared from each strain and analyzed as described in Materials and Methods.

DISCUSSION

A fundamental question in biology is how transmembrane receptors communicate the detection of environmental stimuli to the interior of the cell. Tar, the aspartate receptor of *E. coli*, signals in response to several types of ligands by regulating the activity of its cognate histidine kinase, CheA (*9*). Disulfide-scanning experiments using Tar proteins with Cys substitutions in the first and second transmembrane helices (TM1 and TM2) of Tar (*25*−*28*) strongly suggest that, upon binding of ligands, TM2 moves relative to TM1 and also to the plane of membrane (*28*, *30*−*34*). Here, we have examined how interactions between TM2 of Tar and the phospholipid environment influence the signaling behavior of the receptor.

We focused on the effect of Trp residues that are predicted to localize to the region between the polar headgroups and hydrophobic core of the bilayer. Glycosylation-mapping experiments (*36*) have been used to estimate the position of a transmembrane helix in the dimension perpendicular to the plane of the membrane. Such studies have shown that Trp residues exert a restoring force that can reposition synthetic helices either up or down relative to the membrane surface (*37*, *39*).

We first substituted Ala for Trp-192 and Trp-209, singly and in combination. We chose Ala as the replacement residue because we wanted to avoid introducing a residue with marked chemical properties of its own, such as charge, polarity, a high hydrophobicity index, or a reactive moiety on the side chain. The W192A protein behaved very much

like wild-type Tar in every assay used, with the only consistent difference being a 3-fold increase in the K_i, from 7 μM to 22 μM, in the receptor-coupled CheA kinase assay (Figure 2).

In contrast, the W209A substitution drastically affected the behavior of Tar, decreasing the rate of chemotactic ring migration and eliminating receptor-mediated stimulation of CheA kinase. The WAWA double mutant behaved much like W209A, although chemotactic ring migration was slightly less impaired with the double mutant.

The combination of retained chemotactic ability coupled with lack of CheA stimulation in vitro associated with W209A or WAWA Tar can be explained by the compensatory role of adaptive methylation in vivo. Both proteins showed increased basal levels of methylation but still responded to addition of saturating aspartate (100 mM) and Ni^{2+} (10 mM $NiSO_4$) by increasing and decreasing, respectively, methylation from the altered basal level. Thus, both proteins behave in the absence of ligands as though they had undergone covalent methylation in response to attractant, but they could still mediate qualitatively appropriate responses to attractants and repellents. The tight rings formed by these mutants on aspartate swarm plates could result from a decreased dynamic range of adaptation that traps cells in the steepest portion of the gradient.

The phenotypes of the Trp-substituted mutants can be interpreted as a change in the position of TM2 relative to the membrane, thereby causing a shift in the equilibrium signaling state of the receptor. In the absence of ligand, by default Tar is in the "on" state, which stimulates the CheA kinase. Upon binding of aspartate, TM2 is predicted to slide in an axial fashion toward the cytoplasm to generate the "off" state, in which kinase activity is inhibited. We believe removal of Trp-209, with its affinity for the interfacial region, causes a slight shift of TM2 toward the cytoplasm. We speculate that the most energetically favorable repositioning upon removal of Trp-209 would be a displacement of TM2 similar to when attractant-bound receptor adopts the "off" state. Both of the proposed models for signal transmission through the HAMP linker domain (*54*, *55*) involve tight regulation of the interactions between the HAMP domain and the inner membrane. This linkage could be perturbed by removal of Trp-209.

Using the same reasoning, we predict that the W192A mutation could cause a small shift in the position of the N-terminus of TM2 toward the periplasm, perhaps consistent with the 3-fold increase in the aspartate K_i of the Trp-192 receptor compared with wild type. However, the wild-type level of stimulation of CheA activity and the very slight decrease in basal methylation suggest that no significant changes are imposed on the cytoplasmic domain. Initially, this result may seem contradictory with the changes associated with the W192R mutant receptor (*56*), but the difference presumably lies with the nature of the residue that replaces Trp. Arg would be expected to interact with the negatively charged phospholipid headgroups and thus contribute a specific transmembrane-repositioning effect of its own (*57*). Thus, the W192R substitution may overcome the positioning determinants on the cytoplasmic end of TM2 and cause Tar W192R to stimulate CheA kinase more than the wild-type receptor, in contrast to our observation of a minimal difference between W192A and the wild-type receptor.

To examine how the repositioning of Trp residues within TM2 affects the signaling state of Tar, we moved Trp-209 while leaving Trp-192 in place. If Trp-209 is a primary contributor to the position of TM2 within the membrane, the signaling state of the receptor should be altered when Trp residues are scanned from positions 206 to 212 (Figure 5). Trp residues repositioned toward the periplasm (Trp-206 through Trp-208) should displace TM2 toward the cytoplasm and favor the "off" state (Figure 5B). Trp residues repositioned toward the cytoplasm Trp-210 through Trp-212 should displace TM2 farther into the membrane and favor the "on" state (Figure 5C).

Three of the mutant proteins fulfilled the predictions of our model. W206 and W207 supported reduced but significant chemotaxis in swarm plates (Table 3), failed to stimulate CheA in vitro (Table 4), and showed increased basal levels of methylation (Figure 4). W211 formed wild-type chemotactic swarms, had a modestly increased stimulation of CheA in vitro, and showed normal levels of methylation in vivo. However, the K_i for aspartate in the in vitro assay increased 60-fold (7 to 430 μM) relative to wild-type Tar (Figure 2), and the Hill coefficient dropped from 1.8 to 0.6, indicating that some level of negative cooperativity might operate with the W211 protein. We do not know whether the increased K_i value reflects a lower affinity for aspartate, a partial decoupling of ligand binding and receptor inhibition, or some combination of effects. It is, however, consistent with the notion that moving the Trp residue to a more C-terminal site puts the mutant protein into a signaling conformation that is less subject to inhibition by attractant.

W211 Tar stimulated CheA activity essentially like wild-type Tar. Our prediction that the cytoplasmic end of TM2 should be pulled up into the membrane to mimic repellent-bound receptor had suggested to us that the W211 protein might support a higher rate of CheA autophosphorylation. We note, however, that no one has shown that Tar repellents boost CheA activity in the in vitro receptor-coupled assay. (Ni^{2+} at concentrations that cause a repellent response inhibits CheA activity.)

Cells expressing the W208 and W212 proteins are completely nonchemotactic (Table 3). Their lack of receptor-coupled CheA activity in vitro is shared with the W206, W207, and W210 proteins (Table 4), but the first two receptors differ from the latter three in that those proteins are restored to some level of function in vivo by adaptive methylation. The W208 and W212 proteins are stable when overexpressed (data not shown) and are also present at normal levels in vivo (Figure 4), where they are very highly methylated. In fact, W212 exists solely in the highest methylated form. However, these proteins are not totally inert, since addition of aspartate further increases methylation of the W208 protein, and Ni^{2+} leads to demethylation of both proteins. The W208 and W212 proteins cannot support chemotaxis because their signaling bias is set so far toward CCW that the cells rarely, if ever, tumble (Table 5).

One explanation for the grossly disrupted function of the W208 and W212 receptors is suggested by a helical-wheel projection of TM1 and TM2 of the receptor homodimer (*31*). The side chains of residues Ala-208 and Ile-212 are directed toward TM2 and TM1 of the other subunit, respectively. Insertion of a bulky Trp residue at either of these positions may disrupt the helical packing face, as has been seen in

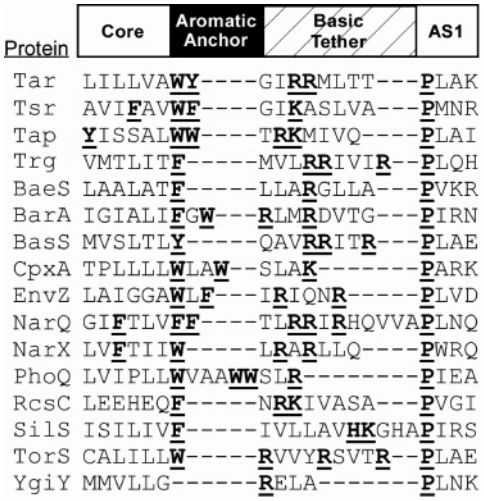

FIGURE 6: Alignment of amino acid sequences of the C-termini of TM2 of chemoreceptors and transmembrane sensor kinases of *E. coli*. All proteins predicted to contain only two TM helices and a P-type linker (*54*) are shown. The conserved Pro residue at the N-terminus of the first amphipathic helix (ASI) of the linker region provided the reference point for the alignment. An evident shared motif consists of one or more aromatic residues that may serve as an anchor within the interfacial zone of the membrane and a basic tether that should interact strongly with negatively charged polar headgroups. The sensor kinases mediate responses to environmental conditions: stress on the cell envelope (BaeS, CpxA, SliS); expression of virulence genes (BarA, PhoQ); biofilm formation (RcsC); environmental osmolarity (EnvZ); use of the alternative electron acceptors nitrate/nitrite (NarQ, NarX) and TMAO (TorS); or sensors of unknown function (BasS, YgiY).

the transmembrane proton channel of the MotAB complex (*58*, *59*) or the dimer−dimer interface in the trimer of dimers in the cytoplasmic domain of the Tsr receptor (*60*). However, other interpretations are equally plausible.

Perhaps the most informative Trp mutant is the double mutant W209A/Y210W. The W210 protein generated by these two substitutions behaves much like W209A. We attribute the signaling abnormalities of the latter protein to the loss of Trp-209. The residue that Trp replaces at position 210 is Tyr. Thus, both the wild-type and W211 proteins have tandem amphipathic aromatic residues (either WYG or AYW at positions 209−211), whereas the W210 and W209A proteins have a single aromatic residue (AWG or AYG, respectively). Preliminary data (Draheim, unpublished) suggest that juxtaposed aromatic residues are required for proper positioning of the cytoplasmic end of TM2.

Bacterial chemoreceptors resemble many members of a large family of homodimeric transmembrane sensor kinases (*54*). Functional chimeras have been made that join the periplasmic, transmembrane, and linker domains of Tar (*61*) and Trg (*62*) to the signaling domain of the sensor kinase EnvZ. In a reciprocal chimera, the periplasmic, transmembrane, and linker domains of the NarX kinase were connected to the signaling and adaptation domains of Tar to create a nitrate/nitrite repellent receptor (*63*). An alignment of the C-terminal portion of TM2 from the four *E. coli* chemoreceptors and all *E. coli* transmembrane sensor kinases with P-type linker domains (Figure 6) reveals that most have one or more aromatic residues closely preceding the highly conserved Pro residue that begins the linker. The function of these aromatic residues, particularly Trp and Tyr, may be to orient the receptor with respect to cytoplasmic face of the cell membrane. Both EnvZ and NarX possess a Trp residue at the cytoplasmic end of TM2.

Our results provide additional evidence of the importance of interactions between TM2 and the surrounding phospholipid environment and demonstrate the crucial role of the Trp residue at the C-terminus of TM2. Such considerations will be important for the design of chemoreceptors and other transmembrane sensors with specific functions. It also appears that tandem aromatic residues may be required for optimal localization of TM2 with respect to the cytoplasmic face of the cell membrane, a possibility that is currently under investigation.

ACKNOWLEDGMENT

Purified CheA, CheW, and our original batch of CheY were generous gifts from John S. Parkinson. Josiah Manson helped with the video analysis of tethered cells. Lily Bartoszek gave the original and revised manuscripts a thorough, professional proofreading. We thank an anonymous reviewer for critical and insightful comments that helped improve the final output. We also thank all members of the Manson laboratory for useful discussion and suggestions.

REFERENCES

1. Tso, W. W., and Adler, J. (1974) Negative chemotaxis in *Escherichia coli*, *J. Bacteriol. 118*, 560−76.
2. Maeda, K., Imae, Y., Shioi, J. I., and Oosawa, F. (1976) Effect of temperature on motility and chemotaxis of *Escherichia coli*, *J. Bacteriol. 127*, 1039−46.
3. Bibikov, S. I., Biran, R., Rudd, K. E., and Parkinson, J. S. (1997) A signal transducer for aerotaxis in *Escherichia coli*, *J. Bacteriol. 179*, 4075−9.
4. Rebbapragada, A., Johnson, M. S., Harding, G. P., Zuccarelli, A. J., Fletcher, H. M., Zhulin, I. B., and Taylor, B. L. (1997) The Aer protein and the serine chemoreceptor Tsr independently sense intracellular energy levels and transduce oxygen, redox, and energy signals for *Escherichia coli* behavior, *Proc. Natl. Acad. Sci. U.S.A. 94*, 10541−6.
5. Mesibov, R., and Adler, J. (1972) Chemotaxis toward amino acids in *Escherichia coli*, *J. Bacteriol. 112*, 315−26.
6. Adler, J., Hazelbauer, G. L., and Dahl, M. M. (1973) Chemotaxis toward sugars in *Escherichia coli*, *J. Bacteriol. 115*, 824−47.
7. Manson, M. D., Blank, V., Brade, G., and Higgins, C. F. (1986) Peptide chemotaxis in *E. coli* involves the Tap signal transducer and the dipeptide permease, *Nature 321*, 253−6.
8. Berg, H. C., and Brown, D. A. (1972) Chemotaxis in *Escherichia coli* analysed by three-dimensional tracking, *Nature 239*, 500−4.
9. Borkovich, K. A., Kaplan, N., Hess, J. F., and Simon, M. I. (1989) Transmembrane signal transduction in bacterial chemotaxis involves ligand-dependent activation of phosphate group transfer, *Proc. Natl. Acad. Sci. U.S.A. 86*, 1208−12.
10. Hess, J. F., Oosawa, K., Kaplan, N., and Simon, M. I. (1988) Phosphorylation of three proteins in the signaling pathway of bacterial chemotaxis, *Cell 53*, 79−87.
11. Ravid, S., Matsumura, P., and Eisenbach, M. (1986) Restoration of flagellar clockwise rotation in bacterial envelopes by insertion of the chemotaxis protein CheY, *Proc. Natl. Acad. Sci. U.S.A. 83*, 7157−61.
12. Welch, M., Oosawa, K., Aizawa, S., and Eisenbach, M. (1993) Phosphorylation-dependent binding of a signal molecule to the flagellar switch of bacteria, *Proc. Natl. Acad. Sci. U.S.A. 90*, 8787−91.
13. Silverman, M., and Simon, M. (1974) Flagellar rotation and the mechanism of bacterial motility, *Nature 249*, 73−4.
14. Turner, L., Ryu, W. S., and Berg, H. C. (2000) Real-time imaging of fluorescent flagellar filaments, *J. Bacteriol. 182*, 2793−801.
15. Cluzel, P., Surette, M., and Leibler, S. (2000) An ultrasensitive bacterial motor revealed by monitoring signaling proteins in single cells, *Science 287*, 1652−5.
16. Borkovich, K. A., and Simon, M. I. (1990) The dynamics of protein phosphorylation in bacterial chemotaxis, *Cell 63*, 1339−48.

17. Goy, M. F., Springer, M. S., and Adler, J. (1977) Sensory transduction in *Escherichia coli*: role of a protein methylation reaction in sensory adaptation, *Proc. Natl. Acad. Sci. U.S.A. 74*, 4964−8.
18. Lupas, A., and Stock, J. (1989) Phosphorylation of an N-terminal regulatory domain activates the CheB methylesterase in bacterial chemotaxis, *J. Biol. Chem. 264*, 17337−42.
19. Springer, M. S., Goy, M. F., and Adler, J. (1977) Sensory transduction in *Escherichia coli*: two complementary pathways of information processing that involve methylated proteins, *Proc. Natl. Acad. Sci. U.S.A. 74*, 3312−6.
20. Milburn, M. V., Prive, G. G., Milligan, D. L., Scott, W. G., Yeh, J., Jancarik, J., Koshland, D. E., Jr., and Kim, S. H. (1991) Three-dimensional structures of the ligand-binding domain of the bacterial aspartate receptor with and without a ligand, *Science 254*, 1342−7.
21. Yeh, J. I., Biemann, H. P., Prive, G. G., Pandit, J., Koshland, D. E., Jr., and Kim, S. H. (1996) High-resolution structures of the ligand binding domain of the wild-type bacterial aspartate receptor, *J. Mol. Biol. 262*, 186−201.
22. Bowie, J. U., Pakula, A. A., and Simon, M. I. (1995) The three-dimensional structure of the aspartate receptor from *Escherichia coli*, *Acta Crystallogr. D 51*, 145−154.
23. Falke, J. J., and Koshland, D. E., Jr. (1987) Global flexibility in a sensory receptor: a site-directed cross-linking approach, *Science 237*, 1596−600.
24. Milligan, D. L., and Koshland, D. E., Jr. (1988) Site-directed cross-linking. Establishing the dimeric structure of the aspartate receptor of bacterial chemotaxis, *J. Biol. Chem. 263*, 6268−75.
25. Lynch, B. A., and Koshland, D. E., Jr. (1991) Disulfide cross-linking studies of the transmembrane regions of the aspartate sensory receptor of *Escherichia coli*, *Proc. Natl. Acad. Sci. U.S.A. 88*, 10402−6.
26. Pakula, A. A., and Simon, M. I. (1992) Determination of transmembrane protein structure by disulfide cross-linking: the *Escherichia coli* Tar receptor, *Proc. Natl. Acad. Sci. U.S.A. 89*, 4144−8.
27. Stoddard, B. L., Bui, J. D., and Koshland, D. E., Jr. (1992) Structure and dynamics of transmembrane signaling by the *Escherichia coli* aspartate receptor, *Biochemistry 31*, 11978−83.
28. Scott, W. G., and Stoddard, B. L. (1994) Transmembrane signalling and the aspartate receptor, *Structure 2*, 877−87.
29. Biemann, H. P., and Koshland, D. E., Jr. (1994) Aspartate receptors of *Escherichia coli* and *Salmonella typhimurium* bind ligand with negative and half-of-the-sites cooperativity, *Biochemistry 33*, 629−34.
30. Danielson, M. A., Biemann, H. P., Koshland, D. E., Jr., and Falke, J. J. (1994) Attractant- and disulfide-induced conformational changes in the ligand binding domain of the chemotaxis aspartate receptor: a 19F NMR study, *Biochemistry 33*, 6100−9.
31. Chervitz, S. A., and Falke, J. J. (1995) Lock on/off disulfides identify the transmembrane signaling helix of the aspartate receptor, *J. Biol. Chem. 270*, 24043−53.
32. Chervitz, S. A., Lin, C. M., and Falke, J. J. (1995) Transmembrane signaling by the aspartate receptor: engineered disulfides reveal static regions of the subunit interface, *Biochemistry 34*, 9722−33.
33. Chervitz, S. A., and Falke, J. J. (1996) Molecular mechanism of transmembrane signaling by the aspartate receptor: a model, *Proc. Natl. Acad. Sci. U.S.A. 93*, 2545−50.
34. Ottemann, K. M., Xiao, W., Shin, Y. K., and Koshland, D. E., Jr. (1999) A piston model for transmembrane signaling of the aspartate receptor, *Science 285*, 1751−4.
35. Yau, W. M., Wimley, W. C., Gawrisch, K., and White, S. H. (1998) The preference of tryptophan for membrane interfaces, *Biochemistry 37*, 14713−8.
36. Nilsson, I., Saaf, A., Whitley, P., Gafvelin, G., Waller, C., and von Heijne, G. (1998) Proline-induced disruption of a transmembrane alpha-helix in its natural environment, *J. Mol. Biol. 284*, 1165−75.
37. Braun, P., and von Heijne, G. (1999) The aromatic residues Trp and Phe have different effects on the positioning of a transmembrane helix in the microsomal membrane, *Biochemistry 38*, 9778−82.
38. Killian, J. A., Salemink, I., de Planque, M. R., Lindblom, G., Koeppe, R. E., 2nd, and Greathouse, D. V. (1996) Induction of nonbilayer structures in diacylphosphatidylcholine model membranes by transmembrane alpha-helical peptides: importance of hydrophobic mismatch and proposed role of tryptophans, *Biochemistry 35*, 1037−45.
39. de Planque, M. R., Bonev, B. B., Demmers, J. A., Greathouse, D. V., Koeppe, R. E., 2nd, Separovic, F., Watts, A., and Killian, J. A. (2003) Interfacial anchor properties of tryptophan residues in transmembrane peptides can dominate over hydrophobic matching effects in peptide-lipid interactions, *Biochemistry 42*, 5341−8.
40. Smith, R. A., and Parkinson, J. S. (1980) Overlapping genes at the cheA locus of *Escherichia coli*, *Proc. Natl. Acad. Sci. U.S.A. 77*, 5370−4.
41. Parkinson, J. S. (1978) Complementation analysis and deletion mapping of *Escherichia coli* mutants defective in chemotaxis, *J. Bacteriol. 135*, 45−53.
42. Weerasuriya, S., Schneider, B. M., and Manson, M. D. (1998) Chimeric chemoreceptors in *Escherichia coli*: signaling properties of Tar-Tap and Tap-Tar hybrids, *J. Bacteriol. 180*, 914−20.
43. Gardina, P., Conway, C., Kossman, M., and Manson, M. (1992) Aspartate and maltose-binding protein interact with adjacent sites in the Tar chemotactic signal transducer of *Escherichia coli*, *J. Bacteriol. 174*, 1528−36.
44. Guzman, L. M., Belin, D., Carson, M. J., and Beckwith, J. (1995) Tight regulation, modulation, and high-level expression by vectors containing the arabinose pBAD promoter, *J. Bacteriol. 177*, 4121−30.
45. Cantwell, B. J., Draheim, R. R., Weart, R. B., Nguyen, C., Stewart, R. C., and Manson, M. D. (2003) CheZ phosphatase localizes to chemoreceptor patches via CheA-short, *J. Bacteriol. 185*, 2354−61.
46. Southern, J. A., Young, D. F., Heaney, F., Baumgartner, W. K., and Randall, R. E. (1991) Identification of an epitope on the P and V proteins of simian virus 5 that distinguishes between two isolates with different biological characteristics, *J. Gen. Virol. 72 (Part 7)*, 1551−7.
47. Miller, J. H. (1972) in *Experiments in Molecular Genetics* p 433, Cold Spring Harbor Laboratory, Cold Spring Harbor, NY.
48. Berg, H. C., and Block, S. M. (1984) A miniature flow cell designed for rapid exchange of media under high-power microscope objectives, *J. Gen. Microbiol. 130*, 2915−20.
49. Gegner, J. A., Graham, D. R., Roth, A. F., and Dahlquist, F. W. (1992) Assembly of an MCP receptor, CheW, and kinase CheA complex in the bacterial chemotaxis signal transduction pathway, *Cell 70*, 975−82.
50. Hess, J. F., Bourret, R. B., and Simon, M. I. (1991) Phosphorylation assays for proteins of the two-component regulatory system controlling chemotaxis in *Escherichia coli*, *Methods Enzymol. 200*, 188−204.
51. Borkovich, K. A., and Simon, M. I. (1991) Coupling of receptor function to phosphate-transfer reactions in bacterial chemotaxis, *Methods Enzymol. 200*, 205−14.
52. Bornhorst, J. A., and Falke, J. J. (2000) Attractant regulation of the aspartate receptor-kinase complex: limited cooperative interactions between receptors and affects of the receptor modification state, *Biochemistry 39*, 9486−93.
53. Bolivar, F., Rodriquez, R. L., Betlach, M. C., and Boyer, H. W. (1977) Construction and characterization of new cloning vehicles. II. A multipurpose cloning system, *Gene 2*, 95−113.
54. Williams, S. B., and Stewart, V. (1999) Functional similarities among two-component sensors and methyl-accepting chemotaxis proteins suggest a role for linker region amphipathic helices in transmembrane signal transduction, *Mol. Microbiol. 33*, 1093−102.
55. Zhu, Y., and Inouye, M. (2003) Analysis of the role of the EnvZ linker region in signal transduction using a chimeric Tar/EnvZ receptor protein, Tez1, *J. Biol. Chem. 278*, 22812−9.
56. Miller, A. S., and Falke, J. J. (2004) Side chains at the membrane-water interface modulate the signaling state of a transmembrane receptor, *Biochemistry 43*, 1763−70.
57. Monne, M., Nilsson, I., Johansson, M., Elmhed, N., and von Heijne, G. (1998) Positively and negatively charged residues have different effects on the position in the membrane of a model transmembrane helix, *J. Mol. Biol. 284*, 1177−83.
58. Sharp, L. L., Zhou, J., and Blair, D. F. (1995) Tryptophan-scanning mutagenesis of MotB, an integral membrane protein essential for flagellar rotation in *Escherichia coli*, *Biochemistry 34*, 9166−71.
59. Sharp, L. L., Zhou, J., and Blair, D. F. (1995) Features of MotA proton channel structure revealed by tryptophan-scanning mutagenesis, *Proc. Natl. Acad. Sci. U.S.A. 92*, 7946−50.

60. Ames, P., Studdert, C. A., Reiser, R. H., and Parkinson, J. S. (2002) Collaborative signaling by mixed chemoreceptor teams in *Escherichia coli*, *Proc. Natl. Acad. Sci. U.S.A. 99*, 7060−5.
61. Utsumi, R., Brissette, R. E., Rampersaud, A., Forst, S. A., Oosawa, K., and Inouye, M. (1989) Activation of bacterial porin gene expression by a chimeric signal transducer in response to aspartate, *Science 245*, 1246−9.
62. Baumgartner, J. W., Kim, C., Brissette, R. E., Inouye, M., Park, C., and Hazelbauer, G. L. (1994) Transmembrane signalling by a hybrid protein: communication from the domain of chemoreceptor Trg that recognizes sugar-binding proteins to the kinase/phosphatase domain of osmosensor EnvZ, *J. Bacteriol. 176*, 1157−63.
63. Ward, S. M., Delgado, A., Gunsalus, R. P., and Manson, M. D. (2002) A NarX-Tar chimera mediates repellent chemotaxis to nitrate and nitrite, *Mol. Microbiol. 44*, 709−19.

BI048969D